Magnetic permeability imaging of metals with a scanning near-field microwave microscope

Sheng-Chiang Lee,[a] C. P. Vlahacos,[b] B. J. Feenstra,[c] Andrew Schwartz,[d] D. E. Steinhauer,[e] F. C. Wellstood, and Steven M. Anlage
Material Research Science and Engineering Center, and Center for Superconductivity Research, Department of Physics, University of Maryland, College Park, Maryland 20742-4111

(Received 27 June 2000; accepted for publication 25 October 2000)

We describe a scanning near-field microwave microscope which uses a loop probe to measure local magnetic properties of metallic samples on a length scale of 200 μm. We demonstrate imaging at 6 GHz through spatiallyresolved ferromagnetic resonance experiments on a single crystal of the colossal magneto-resistive material $La_{0.8}Sr_{0.2}MnO_3$. We find the experimental results are qualitatively and quantitatively well described by a simple model of the system. © *2000 American Institute of Physics.* [S0003-6951(00)03951-6]

The extraordinary increase in the density of magnetic storage media and the access speeds of read/write heads has led to an increased interest in measuring local microwave magnetic properties of materials on short length scales. It is also of interest to evaluate the homogeneity of magnetic properties of samples, such as the local Curie temperature, magnetization, and microscopic phase separation into magnetic and nonmagnetic regions. Many techniques exist to measure the global microwave permeability or susceptibility of materials.[1] Progress has also been made in scanning microscopes which are designed to image radio frequency magnetic fields,[2–4] electron paramagnetic resonance,[5] and ferromagnetic resonance (FMR).[6–9] However, few of these techniques measure microwave permeability on sub-mm length scales.[10,11] To fulfill this need, we have developed a technique for measuring local permeability using a scanning near-field microwave microscope (SNMM). Previously, the SNMM has been used to image conductivity[12] and dielectric properties[13] of materials with an open ended tip probe, which has a maximum electric field and minimum magnetic field at the probe end. In this letter, we discuss the utilization of a short circuited loop probe, which couples magnetically to a sample.

Our SNMM is a driven resonant coaxial transmission line connected to a Cu loop which is formed by shorting the inner conductor of a coaxial cable to the outer conductor.[12–14] We use a frequency following circuit (Fig. 1) and a lock-in amplifier in a feedback loop to lock to one of the resonant frequencies of the coaxial resonator. We then monitor the frequency shift, Δf, due to perturbations from the sample, which is scanned under the probe. By modulating the microwave frequency of the source and monitoring twice the modulation frequency, the losses in the sample contributing to the Q factor of the resonator can be measured[12] as well.

We model the coupling between the loop probe and a sample with the equivalent circuit shown in the inset of Fig. 1. The loop probe is represented as an inductor L_0, the test material as a series combination of its effective inductance L_X and complex impedance $Z_X = R_X + iX_X$, and the coupling as a mutual inductance M. Since the materials of concern are good conductors with a microwave skin depth much smaller than the sample thickness, we model the sample inductance by an identical image of the loop probe, so that $L_X = L_0$. The self-inductance of the loop probe is roughly estimated as $L_0 \approx 1.25\,\mu_0 a$,[15] assuming a circular loop with inner diameter $a \cong$ wire thickness $= 200\,\mu$m. In the high-frequency limit, the surface impedance of the sample can be written as $Z_X = \sqrt{i\mu_0\mu_r\omega\rho}$, where μ_r is the complex relative permeability of the material, ω is the microwave frequency, and ρ is the resistivity of the material, which is considered to be independent of μ_r. Since the loop and its image are roughly circular inductors, we can calculate M as the mutual inductance between two circular loops in the same plane. However, because this two-circular-loop model only approximately describes the geometry, we will ultimately need to treat the value of M as a fitting parameter. The microscope

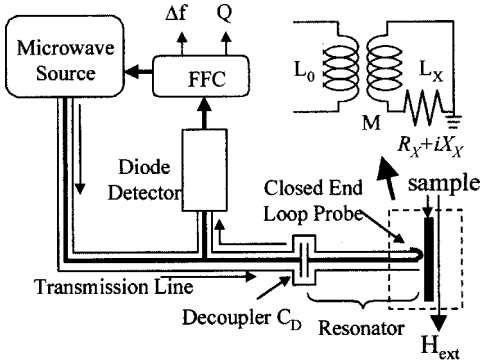

FIG. 1. Schematic of the experimental setup. Inset shows the equivalent circuit representing the interaction between the loop probe and metallic samples.

[a]Electronic mail: sycamore@wam.umd.edu
[b]Present address: NSWC, Carderock, 9500 MacArthur Boulevard, West Bethesda, Maryland 20817-5700.
[c]Present address: Philips Research Labs, Building WB 1-09, Professor Holstlaan 4, 5656 Eindhoven, The Netherlands.
[d]Present address: Neocera, Incorporated, 10 000 Virginia Manor Road, Beltsville, Maryland 20705.
[e]Present address: TriPath Incorporated, 8271 154th Avenue NE, Redmond, Washington 98052.

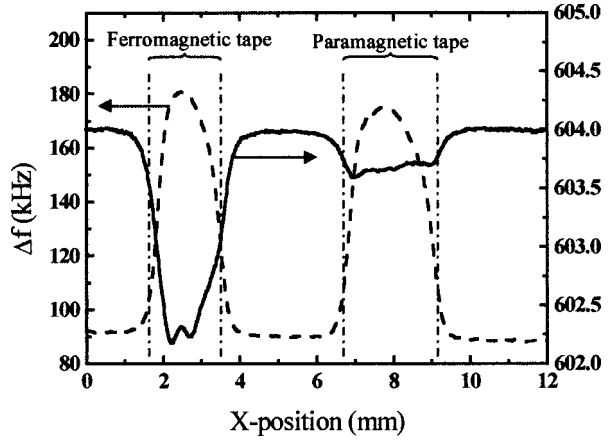

FIG. 2. Line scans of Δf and unloaded Q measurements across a ferromagnetic sample, $Fe_{40}Ni_{40}P_{14}B_6$, and a paramagnetic sample, $Fe_{32}Ni_{36}Cr_{14}P_{12}B_6$ at 6.036 GHz and room temperature. The plane of the loop is aligned with the direction of the scan line at a sample-probe separation of 10 μm measured from the bottom of the probe loop to the surface of the sample. No external magnetic field is applied.

resonator is treated as a transmission line that is capacitively coupled to the microwave source.[12] The frequency shift and Q are calculated using microwave transmission line theory.[12]

In the high-frequency limit, we can take ωL_0 to be much greater than $|Z_X|$. From the equivalent circuit shown in Fig. 1, we find that the load impedance presented by the probe and sample is $Z_{\mathrm{Load}} \cong i\omega L_0(1-k^2)+k^2(R_X+iX_X)$, where the coupling coefficient $k=M/\sqrt{L_0 L_X}$ is a purely geometrical factor. The frequency shift is produced by the imaginary part of Z_{Load}, while the real part of Z_{Load} determines the Q of the microscope.[12,14]

To study the sensitivity of our microwave microscope to magnetic permeability, we measured two metallic glass tapes made of $Fe_{40}Ni_{40}P_{14}B_6$ and $Fe_{32}Ni_{36}Cr_{14}P_{12}B_6$. The difference in composition makes the former ferromagnetic and the latter paramagnetic at room temperature, although both have the same resistivity $\rho = 150\,\mu\Omega$cm. This ensures that any differences observed in images with the microwave microscope are due solely to the differences in permeability.

We measured the samples with both an electric field probe[12,14] and the magnetic field loop probe. With the electric field probe at 5.9 GHz, the two tapes give indistinguishable frequency shift Δf and Q data. However, with the loop probe, the ferromagnetic sample gives a strong reduction in the Q, whereas the Δf data do not show significant contrast (see Fig. 2). To understand why, note that the two metallic glass tapes have similar topography, the coupling k is identical for both materials, and the imaginary part in the second term in the expression for Z_{Load} is small, i.e., $k^2 X_X \ll \omega L_0(1-k^2)$; hence, we do not expect contrast in Δf. However, the significant difference in microwave permeability of the two samples leads to contrast in R_X, which appears as contrast in the microscope Q, consistent with Fig. 2. As a further test, we measured Δf and Q versus the probe-sample separation h, at frequencies of 4.04, GHz, 7.08, and 10.34 GHz. We found an increase in $\Delta f(500\,\mu\mathrm{m}) - \Delta f(10\,\mu\mathrm{m})$ as the frequency increased, and a weak frequency dependence of $Q(500\,\mu\mathrm{m}) - Q(10\,\mu\mathrm{m})$, consistent with the model prediction.

To quantitatively evaluate our theoretical understanding,

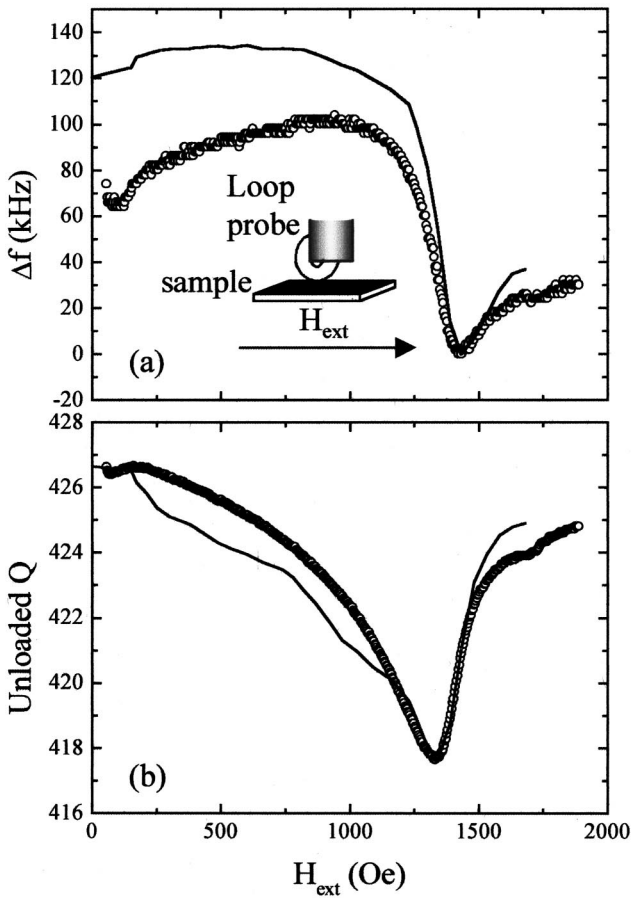

FIG. 3. Measured frequency shift (a) and unloaded Q (b) vs applied magnetic field over a LSMO crystal at a sample-probe separation of 20 μm at 6.037 GHz. Open circles are experimental data; solid line is the model prediction with $Z_X = \sqrt{i\mu_0\mu_r\omega\rho}$ in the model.

we examined a single crystal of the colossal magnetoresistive material $La_{0.8}Sr_{0.2}MnO_3$ (LSMO) in the vicinity of its FMR.[16] The imaging was performed at 301.500 $\pm$ 0.005 K, just below the Curie temperature $T_C = 305.5$ K.[16] With the probe positioned about 20 μm above the center of the sample, we measured Δf and Q as a function of external magnetic field H_{ext} (applied uniformly parallel to the sample surface and the plane of the loop probe, see Fig. 3). In a separate experiment, the complex surface impedance of this sample was also measured.[16,17] FMR is clearly observed as a minimum in $Q(H_{\mathrm{ext}})$ and the point of maximum slope of $\Delta f(H_{\mathrm{ext}})$ in Fig. 3.

We can compare the measured Δf and Q versus H_{ext} of LSMO with our model predictions based on the independently measured complex surface impedance and permeability.[18] In our model, the μ_r dependence only appears in the surface impedance Z_X. To test whether or not this model properly describes the experiment, we evaluated the model with the measured Z_X. It is known from independent information that the decoupler capacitance $C_D \cong 10^{-13}F$, L_0 and $M \cong 10^{-10}H$, and the cable attenuation $0.1 < \alpha < 0.2$ nepers/m, but we treated them as fitting parameters here since none of them were known exactly. We find that the full model prediction fits[19] the experimental results very well with $C_D = 2.94\times10^{-13}F$, $L_0 = 6.5\times10^{-10}H$, $M = 1.3\times10^{-10}H$, and $\alpha = 0.1967$ nepers/m. The data (open circles) and fit (solid line) are shown together in Fig. 3.

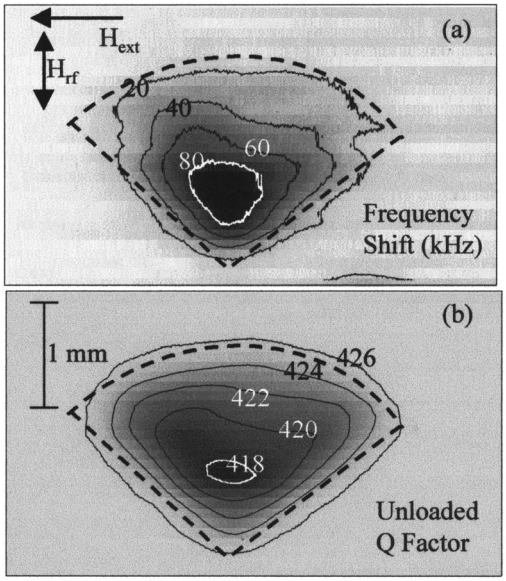

FIG. 4. Images of a LSMO single crystal taken at 6.037 GHz at a sample-probe separation of 10 μm. (a) Δf image of LSMO sample at external field $H_{ext}=1317$ Oe, chosen to give a minimum unloaded Q factor at the center of the sample, and (b) unloaded Q factor image at external field $H_{ext}=1411$ Oe, chosen to give a minimum Δf at the center of the sample. A background frequency shift has been subtracted from (a). The dashed line shows the approximate location of the sample.

We have also developed a technique to image the spatial variation of FMR resonant field in a sample by using either the frequency shift or Q data. To take a FMR image, we fix the homogeneous[20] external magnetic field H_{ext} and record either Δf or Q as a function of position. In Fig. 4(a), $H_{ext} \cong 1317$ Oe is chosen to give the minimum Q in Q versus H_{ext} at the center of the sample, and thus obtain maximum sensitivity in Δf. In a similar fashion, in Fig. 4(b), $H_{ext} \cong 1411$ Oe is chosen to obtain maximum sensitivity in Q. Figure 4(a) shows variations of the local FMR resonant field through the frequency shift, while Fig. 4(b) shows similar spatial variations through Q. Since the frequency shift in Fig. 4(a) and Q in Fig. 4(b) are linearly related to H_{ext} in the vicinity of the fixed H_{ext} (refer to Fig. 3), Figs. 4(a) and (b) can also be converted to variations of FMR resonant field via $\Delta H/\delta(\Delta f) \approx 2.37$ Oe/kHz in Fig. 4(a) and $\Delta H/\Delta Q \approx 25$ Oe/Q in Fig. 4(b). From this we find that the maximum variation of the FMR field in both images is approximately 230 Oe. However, substantial smearing of the image occurs near the sample edges.

The spatial resolution of our microscope is expected to be on the order of the loop diameter when the probe is within one loop diameter of the surface. The loop diameter can be reduced to about 50 μm, and the length of the transmission line resonator can be reduced to 10 cm, with no degradation of signal-to-noise ratio (S/N) in Δf. Further reduction of the loop diameter to 1 μm will improve the spatial resolution, but is also expected to reduce the Δf S/N by a factor of approximately 25.

In conclusion, we have demonstrated the sensitivity of our SNMM to magnetic properties by observing significant contrast between ferromagnetic and paramagnetic materials using a loop probe. Also, we have demonstrated a qualitative and quantitative understanding of FMR data from the system. It should also be possible to extend the technique to image ferromagnetic antiresonance, and antiferromagnetic resonance using the microscope.

The authors thank S. Bhagat for the metallic glass tapes and P. Fournier for help with the susceptibility measurements. The LSMO crystals were grown by Y. Mukovskii and colleagues at the Moscow State Steel and Alloys Institute. This work was supported by the Maryland/NSF MRSEC (NSF DMR-0080008), and the Maryland Center for Superconductivity Research.

[1] V. Korenivski, R. B. van Dover, P. M. Mankiewich, Z.-X. Ma, A. J. Becker, P. A. Polakos, and V. J. Fratello, IEEE Trans. Magn. **32**, 4905 (1996).
[2] R. C. Black, F. C. Wellstood, E. Dantsker, A. H. Miklich, D. T. Nemeth, D. Koelle, F. Ludwig, and J. Clarke, Appl. Phys. Lett. **66**, 99 (1995).
[3] Y. Gao and I. Wolff, IEEE Trans. Microwave Theory Tech. **44**, 911 (1996).
[4] V. Agrawal, P. Neuzil, and D. W. van der Weide, Appl. Phys. Lett. **71**, 2343 (1997).
[5] M. Ikeya, M. Furusawa, and M. Kasuya, Scanning Microsc. **4**, 245 (1990).
[6] Z. Frait, Czech. J. Phys. **9**, 403 (1959); Z. Frait, Czech. J. Phys. **10**, 616 (1960).
[7] Z. Zhang, P. C. Hammel, M. Midzor, M. L. Roukes, and J. R. Childress, Appl. Phys. Lett. **73**, 2036 (1998).
[8] K. Wago, D. Botkin, C. S. Yannoni, and D. Rugar, Appl. Phys. Lett. **72**, 2757 (1998).
[9] S. E. Lofland, S. M. Bhagat, Q. Q. Shu, M. C. Robson, and R. Ramesh, Appl. Phys. Lett. **75**, 1947 (1999).
[10] Y. Martin and H. K. Wickramasinghe, Appl. Phys. Lett. **50**, 1455 (1987).
[11] S. Y. Yamamoto and S. Schultz, Appl. Phys. Lett. **69**, 3263 (1996).
[12] D. E. Steinhauer, C. P. Vlahacos, S. K. Dutta, B. J. Feenstra, F. C. Wellstood, and Steven M. Anlage, Appl. Phys. Lett. **72**, 861 (1998).
[13] D. E. Steinhauer, C. P. Vlahacos, F. C. Wellstood, Steven M. Anlage, C. Canedy, R. Ramesh, A. Stanishevsky, and J. Melngailis, Appl. Phys. Lett. **75**, 3180 (1999).
[14] C. P. Vlahacos, R. C. Black, S. M. Anlage, A. Amar, and F. C. Wellstood, Appl. Phys. Lett. **69**, 3272 (1996).
[15] J. M. Jaycox and M. B. Ketchen, IEEE Trans. Magn. **17**, 400 (1981).
[16] A. Schwartz, M. Scheffler, and S. M. Anlage, Phys. Rev. B **61**, R870 (2000).
[17] A. Schwartz, M. Scheffler, and S. M. Anlage, cond-mat/0010172.
[18] These quantities were measured at the same frequency (6 GHz), and the same temperature (301.5 K) on the same sample described in the paper by A. Schwartz, M. Scheffler, and S. M. Anlage, Phys. Rev. B **61**, R870 (2000). However, since the sample was broken when measured with our microscope, the FMR field was different due to a different demagnetization factor. An offset value for H_{ext} (250 Oe) is used to shift the curves to fit our experimental results.
[19] We fit the model with our data by adjusting these parameters to have a good visual fit. Since C_D and α only affect Q while L_0 and M change both Q and Δf, we varied L_0 and M to fit the $\Delta f(H_{ext})$ data, provided C_D and α are reasonably chosen to give the best visual fit to the $Q(H_{ext})$.
[20] The 2 mm diameter sample is placed in the center of two 5 cm diameter magnet poles which are 1 cm apart.